Brazilian Journal
of Chemical
Engineering

ISSN 0104-6632
Printed in Brazil
www.abeq.org.br/bjche

Vol. 32, No. 03, pp. 795 - 803, July - September, 2015
dx.doi.org/10.1590/0104-6632.20150323s00003642

SYNTHESIS AND CHARACTERIZATION OF SODIUM METHYL ESTER SULFONATE FOR CHEMICALLY-ENHANCED OIL RECOVERY

K. Babu[1], N. K. Maurya[2], A. Mandal[2*] and V. K. Saxena[1]

[1]Department of Chemical Engineering, Indian School of Mines, Dhanbad, India-826 004.
[2]Department of Petroleum Engineering, Indian School of Mines, Dhanbad, India-826 004.
Phone: + 91-326-2235485, Fax: + 91-326-2296632
E-mail: mandal_ajay@hotmail.com

(Submitted: July 16, 2014 ; Revised: December 10, 2014 ; Accepted: December 14, 2014)

Abstract - Attention has been given to reduce the cost of surfactant by using castor oil as an alternative natural source of feedstock. A new surfactant, sodium methyl ester sulfonate (SMES) was synthesised using ricinoleic acid methyl ester, which is obtained from castor oil, for enhanced oil recovery in petroleum industries. The performance of SMES was studied by measuring the surface tension with and without sodium chloride and its thermal stability at reservoir temperature. SMES exhibited good surface activity, reducing the surface tension of surfactant solution up to 38.4 mN/m and 27.6 mN/m without and with NaCl, respectively. During the thermal analysis of SMES, a 31.2% mass loss was observed from 70 °C to 500 °C. The phase behavior of the cosurfactant/SMES-oil-water system plays a key role in interpreting the performance of enhanced oil recovery by microemulsion techniques. Flooding experiments were performed using a 0.5 pore volume of synthesized SMES solutions at three different concentrations. In each case chase water was used to maintain the pressure gradient. The additional recoveries in surfactant flooding were found to be 24.53%, 26.04% and 27.31% for 0.5, 0.6 and 0.7 mass% of surfactant solutions, respectively.
Keywords: Surfactant synthesis; Enhanced oil recovery; Fourier transform infrared spectroscopy (FTIR); Thermal gravimetric analysis (TGA) and Phase behavior.

INTRODUCTION

Enhanced oil recovery (EOR) is meant to improve the sweep efficiency in the reservoir and displacement efficiency by the use of chemicals that reduce the remaining oil saturation below the level achieved by conventional water injection methods. The remaining oil includes both the oil trapped in the flooded areas by capillary forces (residual oil), and the oil in areas not flooded by the injected fluid (bypassed oil). The oil recovered by both primary and secondary processes ranges from 20 to 50 %, depending upon oil and reservoir properties (Awang *et al*., 2008). Chemical flooding methods are classified into a special branch of enhanced oil recovery (EOR) processes to produce residual oil after water flooding. These methods are utilized in order to reduce the interfacial tension, to increase brine viscosity for mobility control and to increase sweep efficiency in tertiary recovery. Surfactants have been considered as good enhanced oil recovery agents since the 1970s (Healy and Reed, 1974) because they can significantly lower the interfacial tensions and alter wetting properties.

The existing commercial surfactants are mostly based on slowly degradable compounds and, in some cases they or their degradation products may become, harmful to the environment or to human beings. The cost of commercial surfactants is also a bottleneck for application in enhanced oil recovery. Many

*To whom correspondence should be addressed

surfactants are produced from natural oils, which can be successfully applied in enhanced oil recovery because of their ability to reduce the interfacial tension to a considerable extent. They should combine a high electrolyte compatibility with high stability to hydrolysis (Elraies *et al*., 2010).

In the present study castor oil was chosen as feedstock for the synthesis of sodium methyl ester sulfonate. Among vegetable oils, castor oil (CO) represents a promising raw material due to its low cost, low toxicity, and its availability as a renewable agricultural resource. CO contains ricinoleic acid (12-hydroxy-cis-9-octadecenoic acid) combining hydroxyl groups and unsaturations (Baber *et al*., 2002). Ricinoleic acid (RA) is present in castor oil up to 85-90%. The hydrogenated form of the fatty acid is ricinoleic acid methyl ester (RAME). The aim of the present investigation is to prepare a castor oil-based sulfonated surfactant (Gregorio *et al*., 2005). The sodium methyl ester sulfonate was prepared by reacting RAME with chlorosulfonic acid. The sulfonated functional group (S=O) was identified in SMES by FTIR analysis. The structural parameters, physicochemical properties and phase behaviour of the synthesized surfactant were also investigated for the purpose of enhanced oil recovery.

MATERIALS AND METHODS

Materials

For surfactant synthesis, laboratory grade chemicals such as chlorosulfonic acid (98%), pyridine (99.5%), ether (99.5%), sodium carbonate (99.5%), sodium bicarbonate (99%) and n-butanol (99.5%) were purchased from Merck Millipore India. Ricinoleic acid methyl ester was purchased from Pasand Speciality Chemicals Rajkot. The acid value, saponification value and iodine values of ricinoleic acid methyl ester are 10-12, 185-190, and 80-90 respectively. Distilled deionized water was used as a solvent for making saturated solutions of the sodium salt.

Synthesis of Sodium Methyl Ester Sulfonate

15 mL of pyridine was added to a 250 mL round bottom (R.B) flask placed in a cooled bath. Then 2.63 g of chlorosulfonic acid was added dropwise to the R.B flask with continuous stirring at 800 rpm for 15 min. A solution of castor oil methyl ester (2.60 g) was added gradually into the mixture and stirred for another 30 min. Then the solution was removed from the ice cooled bath and, when heated at 65 °C, a clear solution appeared. In the second step, aqueous sodium carbonate (33 g) was added in 300 mL of distilled water in an ice cooled bath with constant stirring (800 rpm) and this solution was saturated with inorganic salt by using sodium bicarbonate. The ice cooled saturated solution and heated solution were then quenched and the product was extracted twice into n-butanol (40 mL each) using a separating funnel. The solvent was removed from the crude product by evaporation. The crude product obtained after evaporation was washed with distilled water and petroleum ether to remove organic impurities. Then the crude product was dried at 60 °C under vacuum for 24 hr for further analysis and characterization. The schematic representation of the proposed chemical reaction for SMES surfactant is depicted in Figure 1.

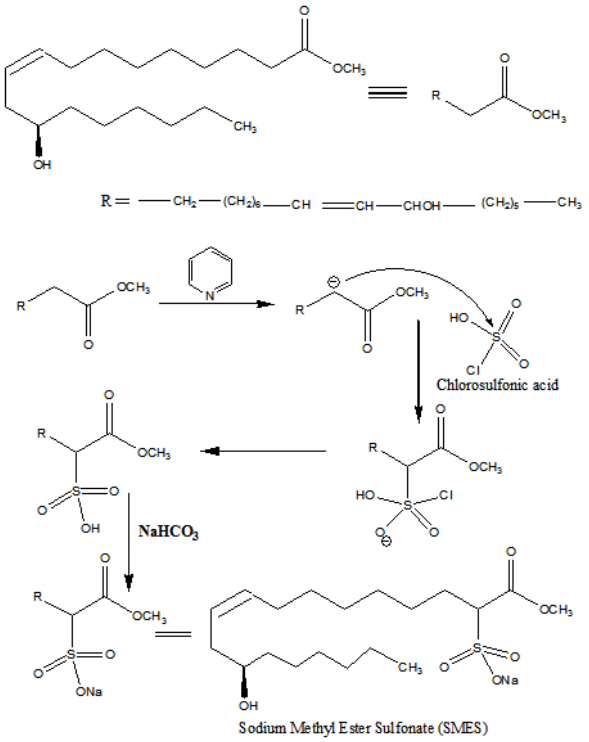

Figure 1: Schematic representation of proposed chemical reaction for SMES surfactant.

FTIR Analysis

The synthesized surfactant was milled with potassium bromide (KBr) to form a fine powder. This powder was then compressed into a thin pallet and analyzed directly. The FTIR spectrophotometer (Perkin Elmer-Spectrum Two) was used to determine the functional group present in the SMES surfactant.

Measurement of Surface Tension

The critical micelle concentration (CMC) and surface tension of SMES surfactant were determined using a DuNoüy ring tensiometer (KRUSS- GmbH-K20 Easy Dyne) at constant temperature (30±0.1 °C). The concentration of the SMES surfactant was varied by dilution of a stock SMES surfactant solution with distilled water using a Hamilton microsyringe. The platinum ring was thoroughly cleaned and flame dried before each measurement. In all cases, more than three successive measurements were carried out. An experiment was also conducted to study the effect of 0.5% to 5% (mass%)sodium chloride on the surface tension of the solution. The measured surface tension values were plotted as a function of SMES surfactant concentration.

Measurement of Thermal Gravimetric Analysis (TGA)

The thermal stability of the synthesized surfactant was measured using a Netzsch-STA 449 Jupiter bench model thermogravimetric analyser (TGA). TGA determines the mass loss of SMES surfactant with temperature. This test was conducted for a temperature range of 29 °C to 500 °C with a heating rate of 23.7 °C/min in a nitrogen environment.

Measurement of Dynamic Light Scattering (DLS)

The particle size analysis of SMES surfactant in aqueous solution was determined using a ZETASIZER (Nano- S90, Nano series Malvern) at 30 ±0.1°C. The laser wavelength was 633 nm and the scattering angle, 90°. The refractive index (1.332) of each solution was measured with a portable refractrometer (refracto 30PX mettler). All samples were prepared in deionized water and filtered using a 0.2 μm pore size membrane to remove possible dust particles from the solution. The absorbances of SMES surfactant solutions were measured using a UV-1800 (UV-VIS spectrophotometer Shimadzu, Japan) at a wavelength of 217 nm. Dynamic light scattering techniques measure the diffusion of particles through the fluid medium and employ the Stoke-Einstein relationship to subsequently determine the size and distribution of micelles.

Construction of Pseudoternary Phase Diagram

The triangular phase diagrams correspond to cuts of a tetrahedron at fixed cosurfactant (n-Hexanol)/SMES surfactant (2:1) mass ratio, so that the apices are n-heptane (oil), water (pseudocomponent) and the cosurfactant/surfactant mixture. The phase diagram was constructed using a conventional titration method. The oil and cosurfactant/SMES surfactant were weighed separately in universal glass bottles. After each addition of a component to a mass mixture of known composition, maintained in a thermostated bath at 30±0.1°C, the sample was homogenized under stirring. Visual observation of the samples with the naked eye allowed determination of the boundary conditions between microemulsion and two phase regions. The samples were stored for 24 hr at constant temperature (30±0.1°C) to achieve equilibrium. After equilibrium was reached, the final visual observations were recorded and the phase diagram was constructed. In our earlier work (Bera *et al*., 2014) it was found that surfactant in the form of microemulsion reduces the IFT more compared to simple surfactant solution.

Conductivity Measurement

The conductivity of the microemulsions was measured using a glass dipping cell with platinum electrodes (Model PCS Testr 35, conductivity meter, Oakton, USA) at 30±0.1°C. The compositions of the microemulsions were taken at different mass ratios of n-heptane: n-hexanol/SMES (0.9:0.1, 0.8:0.2, 0.7:0.3, 0.6:0.4, 0.5:0.5, 0.4:0.6, 0.3:0.7, 0.2:0.8 and 0.1:0.9). The samples were vortexed, sealed with a tight cap and left to attain equilibrium at constant temperature (30±0.1°C) in a water bath. The cell constant was determined using a standard potassium chloride (KCl) solution. Conductivity was measured in a fixed amount of water, stirred to homogenize and then recorded. The other samples were similarly measured.

Surface Morphology

The surface morphology was analysed by FE-SEM SUPRA 55 ZEISS (Germany). The SMES surfactant was maintained in a vacuum oven at 60 °C for 24 hr for moisture reduction and coated with platinum prior to analysis for more accurate results. The charging of samples due to the presence of water is mitigated by the platinum coating.

Flooding Experiments

All the flooding experiments were done by using sand packs in the laboratory. The experimental apparatus is composed of a sand pack holder, cylinders for chemical slugs and crude oil, a positive displace-

ment pump, and measuring cylinders for collecting the samples. The details of the apparatus are available in our earlier paper (Bera *et al*., 2014). The displacement pump is a Teledyne Isco syringe pump. The control and measuring system is composed of different pressure transducers and a computer. The physical model is a homogeneous sand packing model. The model geometry size is L= 43 cm and r= 3 cm.

Sandpack flood tests were employed by (i) preparing uniform sandpacks with 50−80 mesh (ASTM) sand after cleaning and washing with 1% brine. Then the sand was poured into the core holder, which was vertically mounted on a vibrator and filled with 1.0 mass% brine. The core holder was fully filled and vibrated for one hour. (ii) The wet packed sandpack was flooded with brine and the absolute permeability (k_w) calculated. (iii) Then the sand pack was flooded with the crude oil to irreducible water saturation. The initial water saturation was determined on the basis of mass balance. (iv) Water flooding was conducted horizontally at a constant injection flow rate (2 ml/s). The same injection flow rate was used for all the displacement tests of this study. (v) After water flooding, ~0.5 PV surfactant solutions were injected followed by ~2.0 PV water injection as chase water flooding.

RESULTS AND DISCUSSION

FTIR Spectrophotometer of SMES

The infrared spectrum of SMES surfactant is illustrated in Figure 2. The strong band at 1455 cm^{-1} usually corresponds to the asymmetrical bending vibration band of the methyl group (C-H). At the same time, the symmetric and asymmetric C-H stretching modes of the terminal $–CH_3$ group appears at 2873 and 2955 cm^{-1}. The broad vibration centred at 3267 cm^{-1} in SMES is due to OH stretching of the sorbed water. This sorbed water vibration indicated that the surface property of SMES had changed from hydrophobic to hydrophilic (He *et al*., 2004). The strong peak at 1158 cm^{-1} indicates the presence of the sulfonate group (S=O) stretching vibration, which shows that this compound must be sodium methyl ester sulfonate (Silverstein *et al*., 2005). All the IR absorption bands were analysed with reference to the spectrometric identification of organic compounds (Shah *et al*., 1997).

Measurement of Surface Tension

Figure 3a shows the surface tension of SMES surfactant solutions at different concentrations. The critical micelle concentration (CMC) of this surfactant was obtained as the intercept between the descending slope and the constant horizontal line in the surface tension plots against concentration. With increasing concentration of SMES surfactant the values of surface tension decrease continuously until the critical micelle concentration and a minimum surface tension value of 38.4 mN/m was recorded. The surface tension values remained unchanged for concentrations higher than the CMC. In Figure 3b the effect of NaCl concentration on the surface tension of SMES surfactant solution at constant surfactant concentration (CMC) was reported. An increase in the concentration of NaCl decreases the surface tension significantly. The surface tension was reduced to a minimum value of 27.6 mN/m by using sodium chloride.

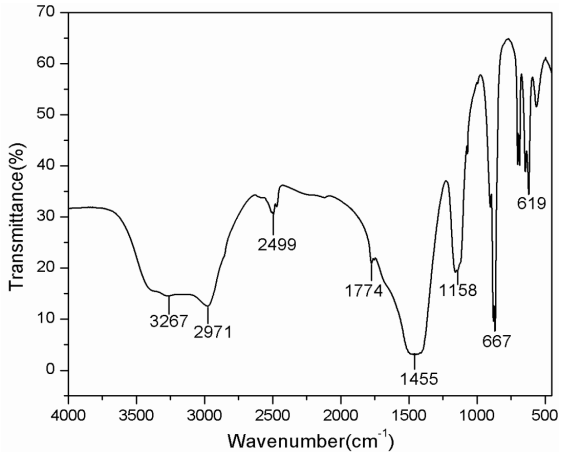

Figure 2: Infrared spectrum of sodium methyl ester sulfonate.

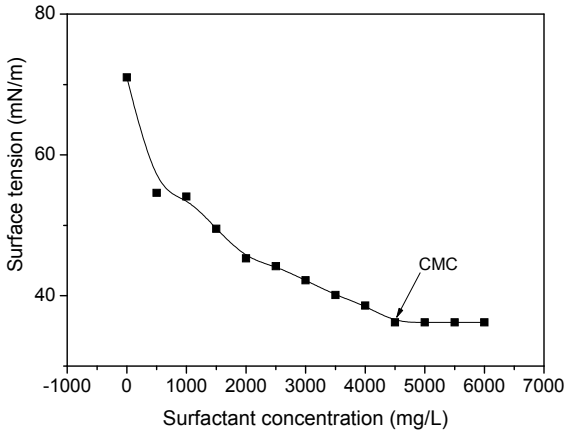

Figure 3a: Surface tension of aqueous SMES surfactant at different concentration.

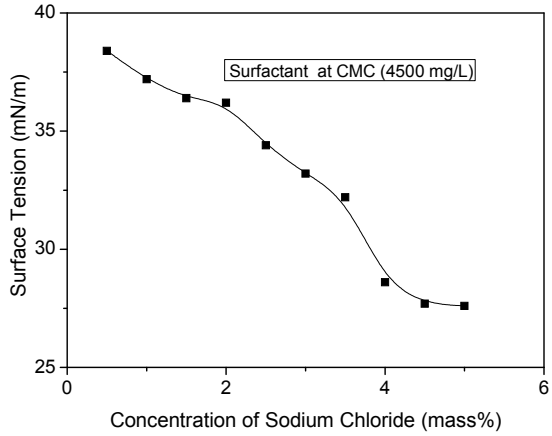

Figure 3b: Influence of sodium chloride concentration on the surface tension of aqueous SMES surfactant at the CMC.

Measurement of TGA

The thermal analysis of SMES surfactant is illustrated in Figure 4. Three mass loss steps were observed. The first region, with a mass loss of 4.4% from ambient to 100 °C corresponds to the loss of weakly bonded water molecules (Carlino *et al*., 1998; Prinetto *et al*., 2000). Then, a 27.6% mass loss occurred sharply in the second region from 100 °C to 150 °C, revealing that SMES molecules start to decompose at temperatures exceeding 100 °C. The third degradation region from 150 °C to 500 °C represents a complex thermal decomposition which may result from addition of the sulfonate group with mass loss of 2.93%; the residual components of SMES surfactant were thermally stable up to 500 °C (Carlino *et al*., 1995; Xi *et al*., 2005). But as the usual reservoir temperatures range between 50 °C to 120 °C, the SMES surfactant should retain an average of 85.91% of its original structure and mass (Zahari *et al*., 2006). It can be concluded that the SMES surfactant is thermally stable under the desired reservoir temperature for the application in enhanced oil recovery.

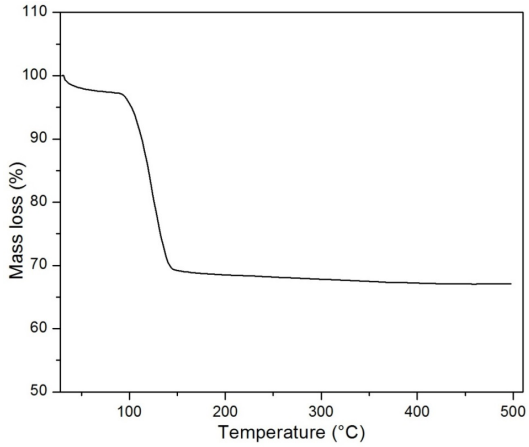

Figure 4: Thermal stability curve for SMES surfactant.

Measurement of Dynamic Light Scattering (DLS)

Figure 5 shows that the hydrodynamic diameter increases with an increase in SMES surfactant concentration. The increase of hydrodynamic diameter results from aggregation of the molecules. Since the rate of diffusion is more rapid for small particles (Kim *et al*., 2004), with the increase in SMES surfactant concentration, the particle size increases simultaneously.

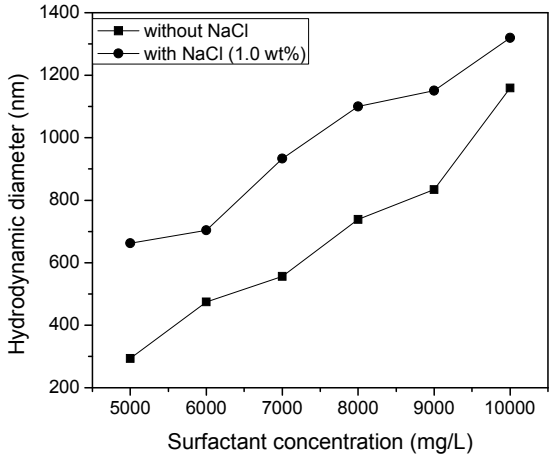

Figure 5: Particle size analysis of SMES surfactant in presence and absence of sodium chloride.

For SMES surfactant solutions the apparent micelle sizes exhibit an increasing trend with increasing concentration of SMES surfactant. (Gracia *et al*.,

2004; Dorsow *et al*., 1983). Figure 5 shows a linear increase of hydrodynamic diameter with surfactant, suggesting that the micelles are in the region of net repulsion.

Pseudoternary Phase Diagram

Figure 6 shows a pseudoternary phase diagram for mixtures of oil, cosurfactant/surfactant and water at various compositions. All types of dispersion, including conventional water in oil and oil in water microemulsion, bicontinuous and transitional liquid crystalline structure with high swelling capacity can be formed by cosurfactant/surfactant (Azira *et al*., 2003). A large microemulsion area (Winsor IV+ Solid) is formed by oil, cosurfactant/surfactant and water (Mo *et al*., 2000). A single phase region (Winsor IV) is observed as the transition occurs from an oil-in-water microemulsion near the water apex to a water–in-oil microemulsion near the n-heptane apex through a bicontinuous structure. The large area of oil in water microemulsion formed by surfactant is due to the large molecular packing ratio of surfactant in the two phase region (Winsor I) (Azira *et al*., 2008; Bera *et al* 2011).

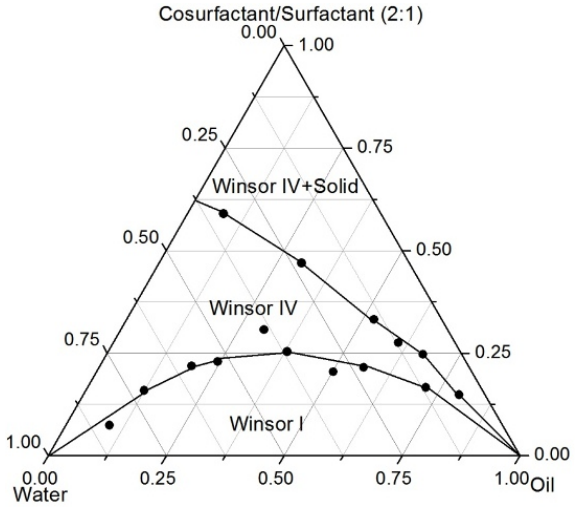

Figure 6: Schematic representation of the pseudoternary phase diagram formed by cosurfactant/surfactant, oil and water mixtures at various compositions (mass fraction).

Conductivity Measurement

The electrical conductivity of the microemulsion with different mass ratios of n-heptane:(n-hexanol/ SMES) was measured in fixed amount of water. Thus, when the surfactant began to aggregate, an increase in conductivity was clearly observed from Figure 7 with a small quantity of Na^+ ions. This result resembles percolation of surfactant aggregation in an isotropic region where the water droplets in the surfactant solution quickly cluster to form an open structure for the efficient transport of Na^+ ions by transient fusion and mass changes. The fraction of miceller head groups neutralized by ions depends only on water molecules. These results are in agreement with the measurement of conductivity, which increases with the degree of miceller ionization (Paul *et al*., 1992; Jada *et al*., 1990; Mukhopadhyay *et al*., 1990).

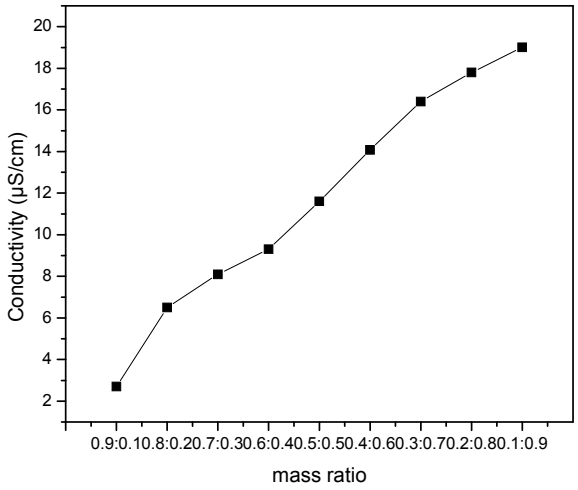

Figure 7: Conductivity with different mass ratios of n-Heptane: (n-Hexanol/SMES surfactant).

Surface Morphology

The surface morphology of the SMES surfactant, examined by FESEM, is shown in Figure 8.

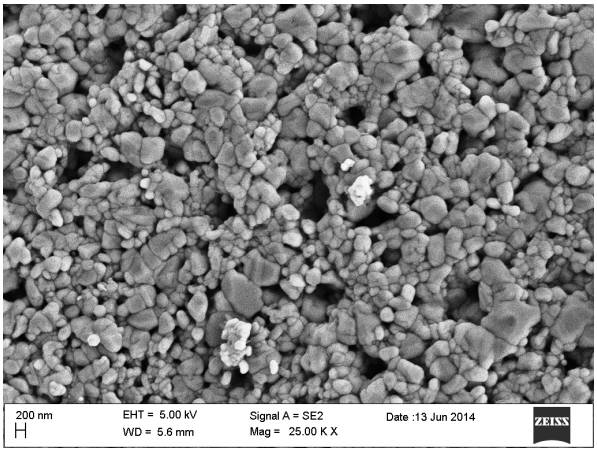

Figure 8: FESEM micrograph of SMES surfactant.

The as synthesized SMES surfactant has an elongated spherical particle structure. The FESEM image illustrates that the particles of the surfactant are in clusters or in an agglomerated form. Also, it can be seen from the figure that the particles have irregular shape and size (Munin *et al*., 2011). The presence of elongated structures suggests that heating at higher temperatures may lead to the formation of the elongated structure seen in the SMES surfactant.

Oil Recovery by Surfactant Flooding

To determine the effects of surfactant concentration on the additional oil recovery, three sets of sandpack floodings (Sample S1, S2 and S3) were conducted using different surfactant concentrations, viz., 0.5, 0.6, and 0.7 mass%. The concentrations of the surfactant were kept above the CMC considering the surfactant loss by adsorption during flooding. Surfactant slugs were injected when the water cut reached ~95% during water flooding. The oil recovery as a function of pore volume injected of surfactant slugs is plotted in Figure 9. Use of surfactant shows significant additional recovery after water flooding due to reduction of the interfacial tension between oil and the displacing fluid and consequent formation of an oil bank. The additional recovery after the water flooding increases with the increase in surfactant concentration. The additional recoveries by surfactant flooding over conventional water flooding are summarized in Table 1. The additional recoveries upon surfactant flooding were 24.53%, 26.04% and 27.31% for 0.5, 0.6 and 0.7 mass% of surfactant solutions respectively. Residual oil saturations were calculated by material balance.

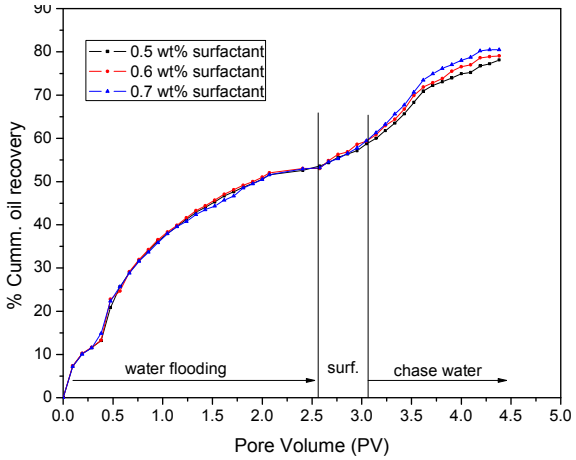

Figure 9: Production performance of SMES Surfactant-Polymer flooding.

Table 1: Recovery of oil by SMES surfactant flooding for three different systems.

Sandpack sample No.	Porosity (%)	Permeability, k (Darcy)		Design of chemical slug for flooding	Recovery of oil after water flooding at 95% water cut (%OOIP)	Additional recovery (% OOIP)	% Saturation		
		k_w (S_w=1)	k_o (S_{wi})				S_{wi}	S_{oi}	S_{or}
S1	8.63	1.27	0.52	0.5 PV 0.5 mass % SMES + Chase water	53.59	24.53	24.28	75.72	16.57
S2	8.52	1.23	0.50	0.5 PV 0.6 mass % SMES + Chase water	53.55	26.04	23.93	76.07	15.52
S3	8.78	1.25	0.52	0.5 PV 0.7 mass % SMES + Chase water	52.53	27.31	23.78	76.22	15.04

CONCLUSION

In the present study sodium methyl ester sulfonate was synthesized from nonedible castor oil for its use as surfactant in enhanced oil recovery. Castor oil is an inexpensive, natural and renewable feedstock and surfactant obtained from it shows good surface active properties. The plot of surface tension at various concentration of surfactant solution exhibits a lowering of surface tension of the surfactant solution down to 38.4 mN/m and 27.6 mN/m without and with NaCl, respectively, at the CMC. The sodium methyl ester sulfonate shows a good thermal stability at reservoir temperature, where a 14.1% mass loss is observed. FTIR spectra confirmed the sulfonate group (S=O) at 1158 cm^{-1} which indicates that this compound must be sodium methyl ester sulfonate. The conductivity of the microemulsion increased with an increase in concentration of surfactant due to Na^+ ions. DLS studies of the aqueous solution of SMES surfactant above the CMC shows that the micelle size increased with increase in concentration of surfactant. From the pseudoternary phase diagram of the oil, cosurfactant/surfactant and water system, three different phases were identified. A large area of oil in water microemulsion (Winsor I) formed by surfactant is an important indication of the use of the surfactant for microemulsion flooding in enhanced oil recovery. Core flooding experiments showed 24.53%, 26.04% and 27.31% additional recovery of crude oil for 0.5, 0.6 and 0.7 mass% of surfactant solutions, respectively, after conventional water flooding.

ACKNOWLEDGEMENT

The Authors thank the Indian School of Mines, Dhanbad, and Department of Chemical Engineering and Petroleum Engineering for financial support for sponsoring this research work. Thanks are also extended to all individuals associated with my research work.

REFERENCES

Awang, M. and Goh, M. S., Sulfonation of phenols extracted from the pyrolysis oil of oil palm shells for enhanced oil recovery. ChemSusChem, 1, 210 (2008).

Azira, H., Assassi, N. and Tazerouti, A., Synthesis of long chain alkanesulfonates by sulfochlorination using sulfuryl chloride. J. Surf. Deterg., 6, 55 (2003).

Azira, H., Tazerouti, A. and Canselier, J. P., Phase behavior of pseudoternary brine/alkane/alcohol-secondary alkanesulfonates systems. Journal of Thermal Analysis Calorimetry, 92, 759 (2008).

Baber, T. M., Vu, D. T. and Lira, C. T., Liquid-liquid equilibrium of the castor oil plus soybean plus hexane ternary system. Journal of Chemical and Engineering Data, 47, 1502 (2002).

Bera, A., Ojha, K., Mandal, A. and Kumar, T., Interfacial tension and phase behavior of surfactant-brine-oil system. Colloids and Surface A Physicochemical and Engineering Aspects, 383, 114 (2011).

Bera, A., Ojha, K., Kumar, T., Mandal, A., Screening of microemulsion properties for application in enhanced oil recovery. Fuel 121, 198-207 (2014).

Carlino, S. and Hudson, M. J., Thermal intercalation of layered double hydroxides capric acid into an Mg–Al LDH. J. Mater Chem., 5, 1433 (1995).

Carlino, S. and Hudson, M. J., A thermal decomposition study on the intercalation of Tris (oxalato) ferrate, trihydrate into a layered (MG AL) double hydroxide. J. Solid State Ionics, 110, 153 (1998).

Dorsow, R. B., Bunton, C. A. and Nicoli, D. F., Comparative study of intermiceller interactions using dynamic light scattering. Journal of Physical Chemistry, 87, 1409 (1983).

Elraies, K. A., Tan, I. M., Awang, M. and Saaid, I., The synthesis and performance of sodium methyl ester sulfonate for enhanced oil recovery. Petroleum Science and Technology, 28, 1799 (2010).

Gracia, C. A., Gomez-Barreiro, S., Gonzalez- Perez, A. and Rodriguez, J. R., Static and dynamic light-scattering studies on miceller solutions of alkyldimethylbenzylammonium chlorides. Journal of Colloid and Interface Science, 276, 408 (2004).

Gregorio, C., Gervajio., Industrial Oil and Fat Products. John Wiley & Sons, Hoboken New Jersey (2005).

He, H. P., Ray, F. L. and Zhu, J. X., Infrared study of $HDTMA^+$ intercalated montmorillonite. Spectrochim Acta, A., 60, 2853 (2004).

Jada, A., Lang, J., Zana, R., Makhloufi, R., Hirsch, E. and Candau, S. J., Ternary water in oil microemulsions made of cationic surfactants, water, and aromatic solvents, droplet sizes and interactions and exchange of material between droplets. J. Phys. Chem., 94, 387 (1990).

Kim, H. U. and Lim, K. H., Sizes and structures of micelles of cationic octadecyl trimethyl ammonium chloride and anionic ammonium dodecyl sulfate surfactants in aqueous solutions. Bulletin of the Korean Chem. Soc., 25, 382 (2004).

Mo, C., Zhong, M. and Zhong, Q., Investigation of structure and structure transition in microemul-

sion systems of sodium dodecyl sulfonate + n-heptane + n-butanol + water by cyclic voltametric and electrical conductivity measurements. J. Electroanal. Chem., 493, 100 (2000).

Mukhopadhyay, L., Bhattacharya, P. K. and Moulik, S. P., Additive effects on the percolation of water/AOT/decane microemulsion with reference to the mechanism of conduction. Colloids Surf., A, 50, 295 (1990).

Munin, A. and Edwards-Lévy, F. Encapsulation of natural polyphenolic compounds. Pharmaceutics, 3, 793 (2011).

Paul, S., Bisal, S. R. and Moulik, S. P., Physicochemical studies on microemulsions: Test of the theories of percolation. J. Phys. Chem., 96, 896 (1992).

Prinetto, F., Ghiotti, G., Graffin, P. and Tichit, D., Synthesis and characterization of sol-gel Mg/Al and Ni/Al layered double hydroxides and comparison with co-precipitated samples. Micropor Mesopor Mat., 39, 229 (2000).

Shah, D. O. and Schechter, R. S., Improved Oil Recovery by Surfactant and Polymer Flooding. Academic Press, New York (1977).

Silverstein, R. M., Webster, F. X. and Kiemle, D. J., Spectrometric Identification of Organic Compounds. John Wiley & Sons, New York (2005).

Xi, Y., Martens, W., He, H. and L Frost, R., Thermogravimetric analysis of organoclays intercalated with the surfactant octadecyl trimethylammonium bromide. Journal of Thermal Analysis and Calorimetry, 81, 91 (2005).

Zahari, I., Arif, A. A., Pauziyah, A. H., Hon, V. Y. and Lim, P. H., Laboratory aspect of chemical EOR processes evaluation for Malaysian oilfields. Paper No. SPE 100943, Asia Pacific Oil and Gas Conference and Exhibition Adelaide, Australia (2006).